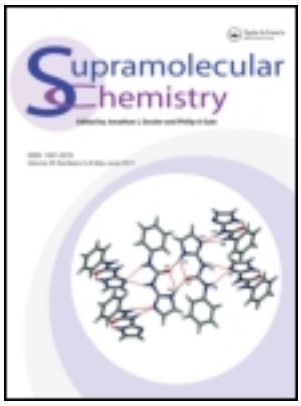

Supramolecular Chemistry
Publication details, including instructions for authors and subscription information:
http://www.tandfonline.com/loi/gsch20

Neutral cryptand-like cyclic peptide-thiourea receptors for selective recognition of sulphate anions in aqueous solvents

Philip G. Young [a], Jack K. Clegg [a b] & Katrina A. Jolliffe [a]

[a] School of Chemistry, The University of Sydney, NSW, 2006, Australia

[b] Department of Chemistry, University of Cambridge, Lensfield Road, Cambridge, CB2 1EW, UK

Available online: 18 Nov 2011

To cite this article: Philip G. Young, Jack K. Clegg & Katrina A. Jolliffe (2012): Neutral cryptand-like cyclic peptide-thiourea receptors for selective recognition of sulphate anions in aqueous solvents, Supramolecular Chemistry, 24:2, 77-87

To link to this article: http://dx.doi.org/10.1080/10610278.2011.622388

Supramolecular Chemistry
Vol. 24, No. 2, February 2012, 77–87

Taylor & Francis
Taylor & Francis Group

Neutral cryptand-like cyclic peptide–thiourea receptors for selective recognition of sulphate anions in aqueous solvents

Philip G. Young[a], Jack K. Clegg[a,b] and Katrina A. Jolliffe[a]*

[a]*School of Chemistry, The University of Sydney, NSW 2006, Australia;* [b]*Department of Chemistry, University of Cambridge, Lensfield Road, Cambridge CB2 1EW, UK*

(*Received 29 June 2011; final version received 31 August 2011*)

The synthesis and anion complexation properties of two hybrid cyclic peptide–thiourea cryptands have been studied. Receptors encapsulate sulphate via nine hydrogen bonds and show selectivity for this anion in solvent mixtures containing up to 20% H_2O/deuterodimethyl sulphoxide. In this solvent mixture, chloride, bromide and acetate are encapsulated via six hydrogen bonds and with lower affinity than sulphate.

Keywords: anion recognition; thiourea; cyclic peptide; sulphate

Introduction

Anions are critical to the maintenance of life, with almost every biochemical process involving the recognition, transport or transformation of anions at some point. This crucial role has led to growing interest in the design of artificial anion receptors for sensing applications in biochemistry and biomedicine (as well as for environmental applications) (*1*). However, the development of anion receptors that operate with high selectivity and affinity in aqueous solution remains a challenge (*2*).

To achieve the necessary substrate affinity and selectivity for biological function, nature uses a number of efficient binding motifs including defined arrays of convergent hydrogen-bond donors positioned inside a cavity or cleft that is well shielded by solvent molecules. Such arrangements are found in both phosphate- and sulphate-binding proteins with an additional hydrogen-bond acceptor present in the phosphate-binding protein that is considered to be responsible for the high phosphate selectivity of this protein (*3*). Synthetic receptors frequently employ either electrostatic interactions, hydrogen bonds or a combination of these for anion recognition (*4*). While significant advances have recently been made in the development of synthetic receptors capable of binding anions in aqueous solutions by strong electrostatic interactions (*5*), those capable of binding anions with high selectivity and affinity through hydrogen-bonding interactions in polar, and particularly aqueous, solvents are rare (*6*, *7*). One reason for this is the high free energies of hydration of many anions, which require design of receptors that are able to compete with the hydrogen-bonding ability of water and other polar solvents. In this regard, tetrahedral anions, such as sulphate ($\Delta G = -1080\,\mathrm{kJ\,mol^{-1}}$) (*8*), are particularly challenging targets and it is only relatively recently that synthetic receptors capable of binding sulphate ions in aqueous mixtures have been described (*7*).

One approach to the development of neutral receptors for anions in aqueous mixtures is to mimic the approach observed in the sulphate- and phosphate-binding proteins. The positioning of well-organised hydrogen-bond donors about a cleft or cavity has recently been employed in a number of receptors to great effect (*9*). Amides, ureas and thioureas are frequently employed to provide hydrogen-bond donor sites (*10*), and the use of either ureas or thioureas in combination with amides has been shown to provide significant enhancements in anion binding affinity (*11*). We recently reported the design and the synthesis of two cryptand-like hybrid amide–thiourea anion receptors (**1** and **2**) together with their anion binding capabilities in 0.5% v/v H_2O/deuterodimethyl sulphoxide (DMSO-d_6) (*12*). In this solvent, receptor **1** showed strong binding of both acetate and chloride ions (both $K_a > 10^4\,\mathrm{M^{-1}}$), while receptor **2** was selective towards acetate ions ($K_a > 10^4\,\mathrm{M^{-1}}$). We report here further anion binding studies with these compounds including the binding of sulphate ions in mixed water–DMSO solutions by receptor **1**.

Results and discussion

Synthesis of compounds 1 and 2

Receptors **1** and **2** are based on the structures of naturally occurring Lissoclinum cyclic peptides (*13*), which contain azole heterocycles alternating with amide bonds,

*Corresponding author. Email: kate.jolliffe@sydney.edu.au

ISSN 1061-0278 print/ISSN 1029-0478 online

http://dx.doi.org/10.1080/10610278.2011.622388
http://www.tandfonline.com

providing a series of alternating hydrogen-bond donors and acceptors that line the interior of the macrocycle and form a network of bifurcated hydrogen bonds. This provides relatively rigid scaffolds suitable for application as molecular receptors (*14*). We initially envisaged that the amide hydrogen-bond donors in the cyclic peptide macrocycles (*15*) would complement those in the thiourea side chains in **1** and **2** to provide a 'nest' of nine hydrogen-bond donors for anion binding. However, our initial studies provided conflicting results with the amide NH proton NMR signals of **1** shifting upfield upon anion binding while those of **2** shifted downfield (*12*). Our present studies were carried out to further investigate this and to determine how anions bind to these receptors.

In our initial syntheses of **1** and **2**, we condensed the tripodal cyclic peptide amine **3** with tris-isothiocyanates derived from tren (**4**) and 1,3,5-triethyl-2,4,6-triaminomethylbenzene (**5**). In order to investigate whether improved yields of **1** and **2** could be obtained by reversing the functionality of the coupling partners, we prepared the cyclic peptide tris-isothiocyanate **6** in excellent yield upon treatment of the known tris-hydrobromide salt **3a** with triethylamine and carbon disulphide in the presence of *N,N′*-dicyclohexylcarbodiimide (DCC) as a desulphurising agent (Scheme 1). This was then condensed under high dilution conditions with either triamine **7** or **8** to provide the required cryptands, albeit in lower yields to those obtained from the reverse coupling partners under identical conditions.

X-ray crystal structure analysis of 6

Single crystals of **6**, appropriate for X-ray diffraction studies, were obtained from slow crystallisation in dichloromethane/ethyl acetate solution (Figure 1). Tris-isothiocyanate **6** crystallises in the chiral monoclinic space group *C*2 with one molecule in the asymmetric unit. Although the quality of data obtained is not ideal, it is more than sufficient to establish connectivity of the structure. The refined Flack parameter (*16*) [−0.10 (18)] confirms the enantiopurity of the structure. In a similar manner to the previously reported structures of **1** and **2** (*12*), each molecule features an almost planar macrocyclic structure wherein one of the three oxazole rings is tilted slightly out of the plane that is stabilised by intramolecular hydrogen-bonding interactions (Table 1).

The three modified ornithine side chains all project from one side of the macrocyclic scaffold. Interestingly, two molecules of **6** pack together so that one isothiocyanate arm from each molecule is directed towards the centre of the macrocycle of the adjacent peptide (Figure 2) with weak hydrogen-bonding interactions (NH···S = 3.05–3.25 Å) present between peptide amide protons and the sulphur atom. Given the similarities in peptide conformation observed in the X-ray crystal structures of **1**, **2** and **6**, this interaction suggested to us that the amide NHs of the cyclic peptide 'floor' could play a significant role in anion binding in cryptands **1** and **2**.

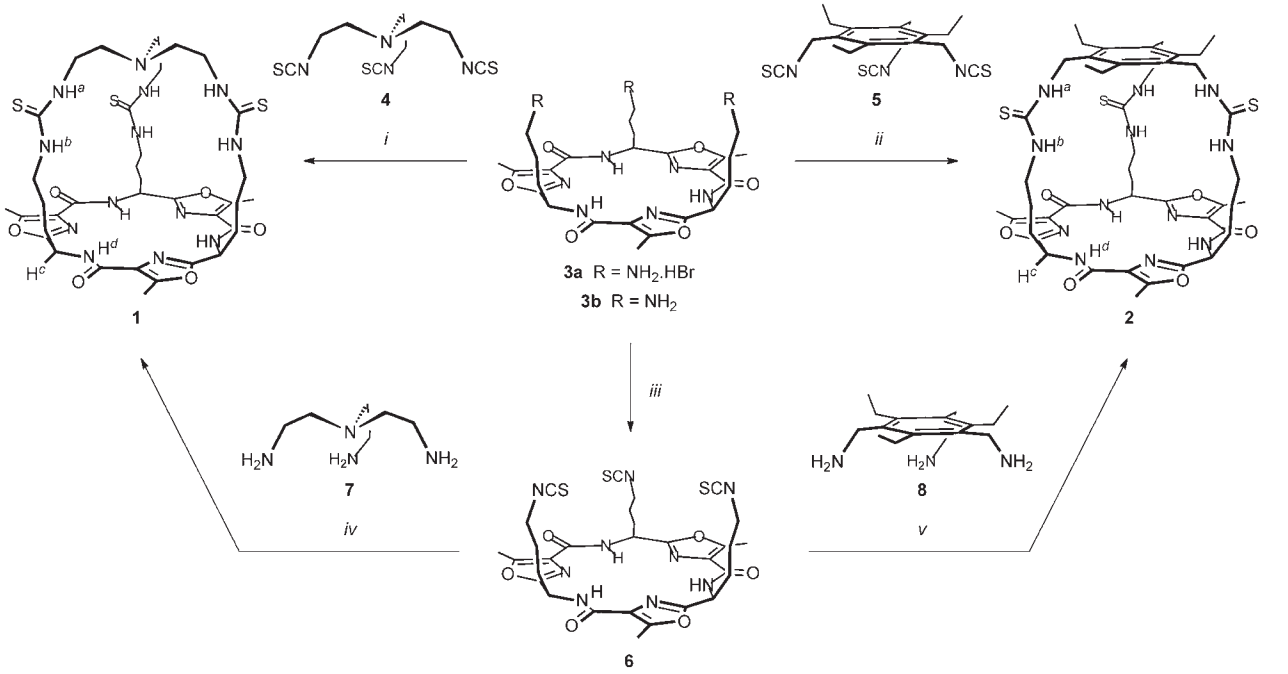

Scheme 1. Synthesis of compounds **1** and **2**. Reagents and conditions: (i) **3a**, $CHCl_3$, 54% or **3b**, triethylamine, $CHCl_3$, DMF, 62%; (ii) **3a**, $CHCl_3$, 69% or **3b**, triethylamine, $CHCl_3$, DMF, 50%; (iii) CS_2, *N,N′*-DCC, triethylamine, DMF, 84%; (iv) **6**, $CHCl_3$, 42% and (v) **6**, $CHCl_3$, 16%.

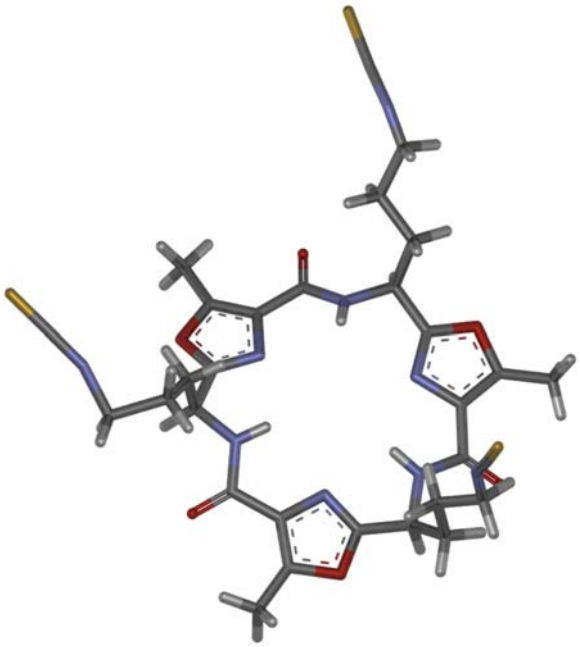

Figure 1. Schematic representation of the crystal structure of **6**. Regions of disorder are removed for clarity.

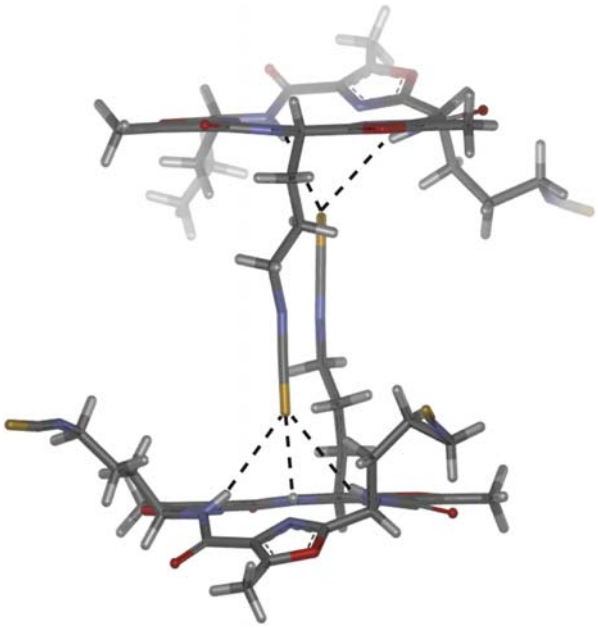

Figure 2. Schematic representation of part of the crystal packing in **6**. Regions of disorder are removed for clarity. Dashed lines indicate hydrogen bonds.

Each of these hydrogen-bonded dimers interacts with adjacent molecules through two sets of intramolecular interactions. Firstly, the two planar oxazole groups interact with each other in an intermolecular fashion via offset face-to-face $\pi-\pi$ stacking indicated by centroid–centroid distances of 3.6 and 3.7 Å (Figure 3, left). In combination with the intermolecular hydrogen-bonding interactions just discussed, this results in the formation of infinite 1D chains of molecules that propagate along the crystallographic *a*-axis. Each of these chains undergoes further supramolecular bonding with neighbouring chains via methyl–oxazole π interactions with a centroid–methyl carbon distance of 3.58 Å. These interactions extend parallel to the crystallographic *b*-axis. The net effect of all these interactions is the formation of infinite 2D sheets of molecules that extend parallel to the crystallographic *ab*-plane.

Anion binding evaluations of 1 and 2

Preliminary anion binding studies with **1** and **2** carried out by titration with tetrabutylammonium salts with a range of anions in 0.5% v/v H_2O/DMSO-d_6 have been communicated previously (*12*) and are summarised in Table 2 together with additional data from the present study. Our initial studies indicated that acetate anions bound strongly to both receptors with apparent stability constants $(K_a) > 10^4\,M^{-1}$. The tren-capped cryptand **1** also displayed strong binding affinity for chloride and bromide ($K_a > 10^4$ and $2.6 \times 10^3\,M^{-1}$, respectively), whereas binding of these anions with **2** was markedly weaker ($K_a = 87$ and $11\,M^{-1}$, respectively). We hypothesised that the ability of the tren-capped **1** to bind a greater range of anions than **2** is a result of the increased flexibility of the aliphatic capping unit of the molecule compared to the rigid 1,3,5-triethylbenzene cap of **2**. In order to investigate this effect and to further probe the binding modes of the two cryptands, additional binding studies were conducted

Table 1. Hydrogen-bond geometry.

Donor	Hydrogen	Acceptor	D-H (Å)	H-A (Å)	D–A (Å)	DHA (°)
N(2)	H(2)	N(1)	0.88	2.31	2.739(8)	110.4
N(2)	H(2)	N(4)	0.88	2.28	2.705(9)	109.2
N(5)	H(5)	N(4)	0.88	2.39	2.786(9)	107.3
N(5)	H(5)	N(7)	0.88	2.40	2.745(9)	103.3
N(8)	H(8)	N(1)	0.88	2.52	2.755(8)	95.8
N(8)	H(8)	N(7)	0.88	2.37	2.754(9)	106.7

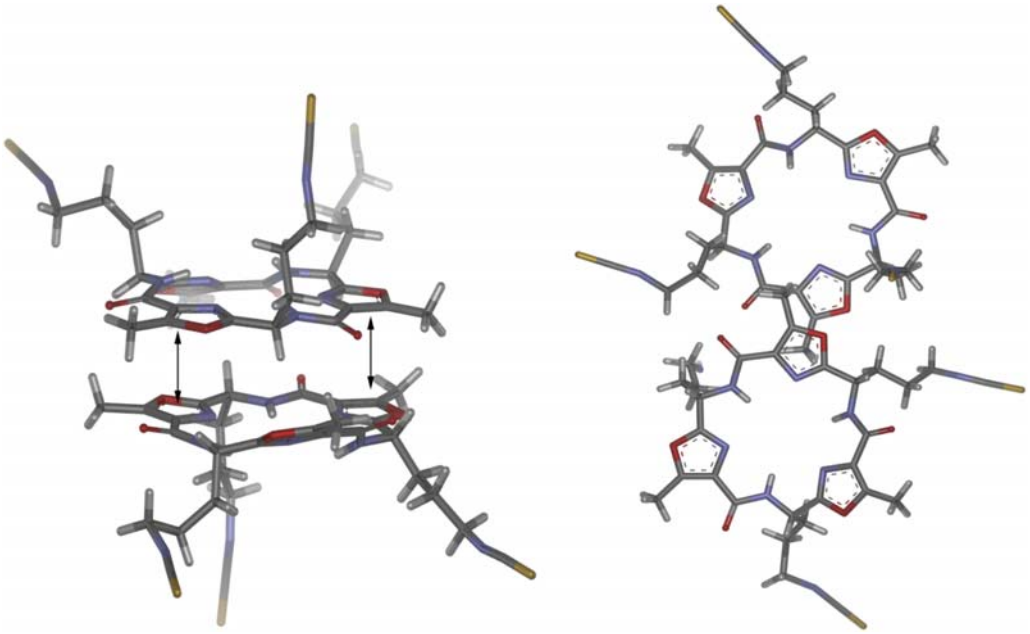

Figure 3. Schematic representation of sections of the crystal packing in **6**. Left: dimers formed via oxazole–oxazole $\pi-\pi$ interaction (double-headed arrows indicate $\pi-\pi$ interactions). Right: dimers formed from weak methyl–oxazole interactions. Regions of disorder are removed for clarity.

with a larger range of anions. Specifically, we chose to investigate binding with benzoate (BzO^-), tosylate (TsO^-) and sulphate (SO_4^{2-}) (each added as their tetrabutylammonium salts).

As observed in our previous studies, the addition of anions to both **1** and **2** resulted in downfield shifts of the thiourea NH proton signals, indicative of fast exchange processes (in all cases except for the addition of sulphate to **1**; see below), which were fit to a 1:1 binding model to give apparent stability constants (see supporting information for fitted titration data). Representative spectra for titrations of **1** and **2** with acetate ions are shown in Figure 4, illustrating the significant downfield shifts of the thiourea proton signals [$\Delta\delta = 0.75$ and 0.85 parts per

Table 2. Apparent stability constants (K_a/M^{-1}) of various anions (added as their tetrabutylammonium salts) with **1** and **2** as determined by monitoring the thiourea proton resonances, NH^a and NH^b, and amide proton resonances, NH^d, during ^1H NMR titrations in 0.5% H_2O/DMSO-d_6.[a]

	Receptor 1[b]		Receptor 2[c]	
Anion guest	Thiourea NHs	Amide NH	Thiourea NHs	Amide NH
Cl^-	$>10^4$[d]	$>10^4$	87[d]	89
Br^-	2.7×10^3[d]	1.6×10^3	11 ($\pm$6)[d]	17
I^-	<10[d]	<10	<10[d]	<10
NO_3^-	<10[d]	<10	<10[d]	<10
AcO^-	$>10^4$[d]	$>10^4$	$>10^4$[d]	$>10^4$
$H_2PO_4^-$	—[e]	—[e]	—[e]	$>10^4$
HSO_4^-	<10[d]	<10	<10[d]	<10
BzO^-	307	<10	—[f]	—[f]
TsO^-	<10	<10	<10	<10
SO_4^{2-}	$>10^4$[g]	$>10^4$[g]	$>10^4$	$>10^4$

[a] Data were fit to a 1:1 binding model. For thiourea protons, the K_a values are an average of the values obtained by monitoring NH^a and NH^b. Errors $<15\%$ unless specified.
[b] Determined at 330 K.
[c] Determined at 300 K.
[d] Data from Ref. (*12*).
[e] Peak broadening prevented an apparent stability constant from being determined.
[f] Titration data from NH^a and NH^b did not give consistent apparent stability constants.
[g] Titration displayed slow exchange on the NMR timescale.

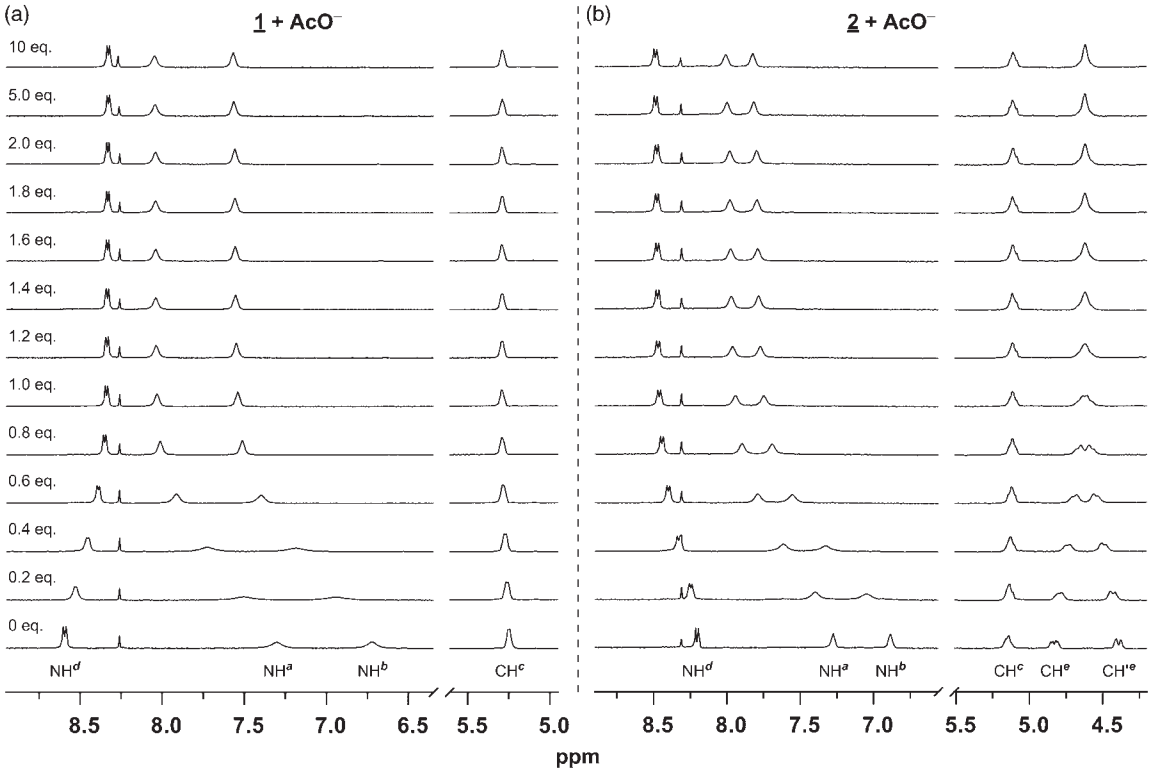

Figure 4. Selected partial ^{1}H NMR (400 MHz, 0.5% v/v H_2O/DMSO-d_6) titration spectra from titrations with tetrabutylammonium acetate with **1** (330 K) (left) and **2** (300 K) (right).

million (ppm) for **1** and 0.73 and 0.94 ppm for **2**, respectively]. In most cases, shifts were also observed for the signals attributable to the amide NH protons. The addition of anions to **2** resulted in a downfield shift of this signal (Figure 4(b)). Fitting the chemical shift data for this signal to a 1:1 binding model gave apparent stability constants consistent to those obtained from the thiourea NH protons (within experimental error) and notably allowed us to determine a binding constant for $H_2PO_4^-$ ($K_a > 10^4\,M^{-1}$), which could not be obtained by monitoring thiourea protons due to line broadening. In contrast, the signal attributable to the amide NH of **1** shifted upfield upon addition of anions (Figure 4(a)) with the exceptions of benzoate and sulphate (see below). This chemical shift data could also be fit to a 1:1 binding model to give apparent stability constants consistent with those obtained from thiourea protons.

We attribute opposite changes in chemical shifts to the relative flexibility of the two cryptands – the upfield shifts of the amide protons of **1** can be attributed to weakening of the network of hydrogen-bonding interactions between these protons and oxazole nitrogens which may be required to allow the molecule to adopt a conformation to accommodate anions. The greater flexibility of the tren cap of **1**, in comparison to the benzene cap of **2**, provides the cryptand with slightly greater overall conformational freedom, allowing greater twisting of the peptide macrocycle in this case.

Notably, in the case of addition of benzoate to **1**, while the thiourea NH signals undergo the expected downfield shifts indicative of anion binding ($K_a = 307\,M^{-1}$), the chemical shift of the signal attributable to the amide protons does not change over the course of titration (Figure 5). This provides useful information about the mode of binding of anions to **1**, suggesting that benzoate binds in a different mode to the other anions investigated. Benzoate is too large to fit inside the cavity of **1** and is likely to bind to the thiourea side chains on the outside of the cryptand. This would result in minimal perturbation of the cyclic peptide structure and explains the absence of movement of the signal attributable to the amide protons in this case. In contrast, anions such as acetate and chloride can fit inside the cryptand, resulting in structural changes to the cyclic peptide scaffold of **1**, which are reflected by upfield shifts of amide proton signals.

In contrast to all other systems investigated, when sulphate ions were added to receptor **1**, slow exchange processes were observed with the gradual appearance of new peaks corresponding to a host–guest complex in the ^{1}H NMR spectra (Figure 6). As previously noted for the titration of **1** with acetate (Figure 4(a)), a significant downfield shift of thiourea protons (NH^a and NH^b) was

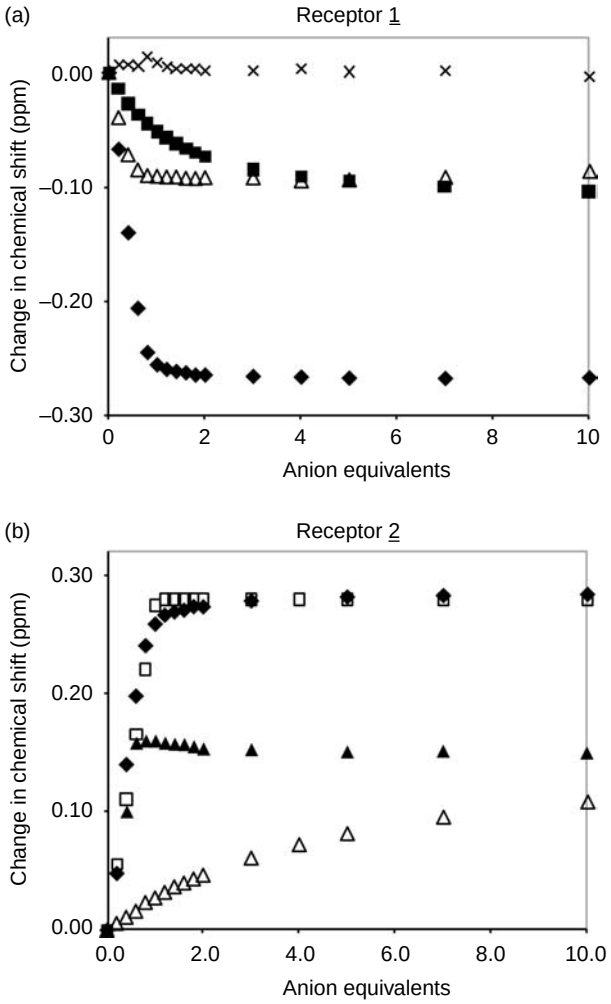

Figure 5. Changes in chemical shift (ppm) of the amide protons of (a) **1** and (b) **2** in 0.5% v/v H_2O/DMSO-d_6 with the addition of various anions (keys: × = benzoate, ■ = bromide, △ = chloride, ◆ = acetate, □ = dihydrogen phosphate, ▲ = sulphate).

observed with the addition of sulphate ($\Delta\delta = 1.85$ and 2.17 ppm, respectively). Upon addition of one equivalent of sulphate ions to **1**, complete conversion to the host–guest complex was observed.

However, in sharp contrast to upfield shifts of the amide proton signals of **1** (NH^d) observed upon addition of all other anions (Figure 4(a)), this signal shifted downfield from 8.60 to 9.39 ppm ($\Delta\delta = 0.79$ ppm) on addition of sulphate. The large downfield shift of the amide protons is strong evidence that amide protons contribute significantly to binding of sulphate, in contrast to the binding behaviour observed for **1** with all other anions investigated, where the amide NH does not appear to be involved in anion binding. A comparison of the previously reported X-ray crystal structure of **1** with that of **6** (Figure 3), which indicates that the cyclic peptide amide protons are involved in weak hydrogen bonding to the isothiocyanate sulphur atom, suggests that the cyclic peptide backbone of **1** adopts a similar conformation with amide hydrogens pointing up towards the centre of the cryptand cavity (*12*). We postulate that a total of nine hydrogen bonds act to hold a central sulphate oxoanion within the cavity of **1**, as depicted in Figure 7(a). In contrast, the titration data obtained for chloride, bromide and acetate ions suggest that a maximum of six hydrogen bonds from the thiourea groups contribute to binding an encapsulated guest (Figure 7(b)), while benzoate binds outside the cavity (Figure 7(c)). The complementary size and shape of **1** for sulphate permit each thiourea binding site to donate two hydrogen bonds to individual oxygen atoms which leaves a further three contributions from the peptide backbone to complete the coordination network. The association constant found for hydrogen sulphate ($K_a < 10\,M^{-1}$) suggests that the anion is not able to adopt a binding mode like that represented in Figure 7(a) due to its higher protonation state and, as such, is not bound with any observable affinity. In this regard, **1** is able to distinguish anion guests based not only on their size but also on protonation states.

While both **1** and **2** bind sulphate strongly ($K_a > 10^4\,M^{-1}$), the chemical shift data suggest that the peptide backbone of **2** ($\Delta\delta = 0.16$ ppm) does not play an important role in the recognition of sulphate as that of **1** ($\Delta\delta = 0.79$ ppm). This is attributed to the increased rigidity of **2** relative to **1**, which restricts additional binding interactions from the peptide backbone. Indeed, the ability of cryptand **1** to bind strongly to a wider range of anionic substrates, compared to **2**, suggests that **1** is able to accommodate guests through an induced-fit mechanism made possible by the flexible nature of its aliphatic capping unit.

Due to the large apparent stability constants obtained for **1** and **2** with a range of anions in 0.5% v/v H_2O/DMSO-d_6 and the interesting results observed for binding of sulphate ions, we chose to investigate anion binding in more competitive media. Unfortunately, further attempts to investigate the binding selectivity of **2** were restricted by the low solubility of the receptor in more competitive solvent mixtures. However, the solubility of **1** in higher ratios of water in DMSO-d_6 allowed binding studies to be carried out so that the selectivity of the receptor towards the most strongly bound anions (i.e. chloride, bromide, acetate and sulphate) could be ascertained.

Table 3 summarises the apparent stability constants found for **1** for titrations performed in 10, 20, 25 and 35% v/v H_2O/DMSO-d_6 mixtures. In all cases, moving to the more competitive media resulted in fast exchange processes on the NMR timescale as evidenced by time-averaged signals for each proton environment of **1**.

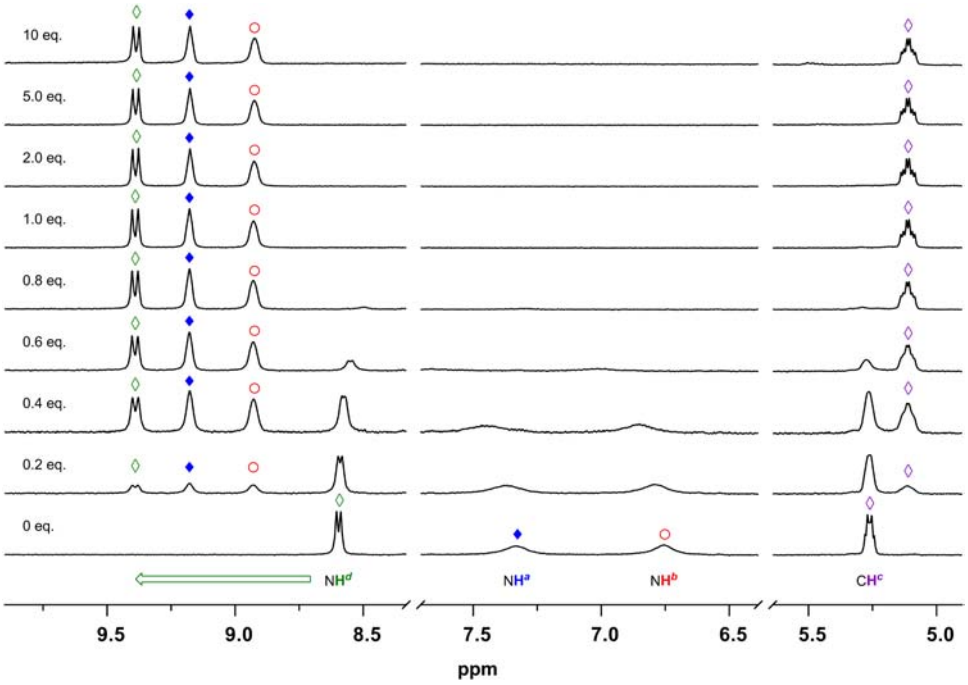

Figure 6. Selected ^{1}H NMR (400 MHz, 330 K) titration spectra from titrations with bis(tetrabutylammonium) sulphate with **1** in 0.5% v/v H_2O/DMSO-d_6. Slow exchange processes were observed.

In 10% v/v H_2O/DMSO-d_6, appreciable reductions in apparent stability constants were observed for chloride, bromide and acetate ions, while sulphate again provided an apparent stability constant of $>10^4\,M^{-1}$ (Table 3).

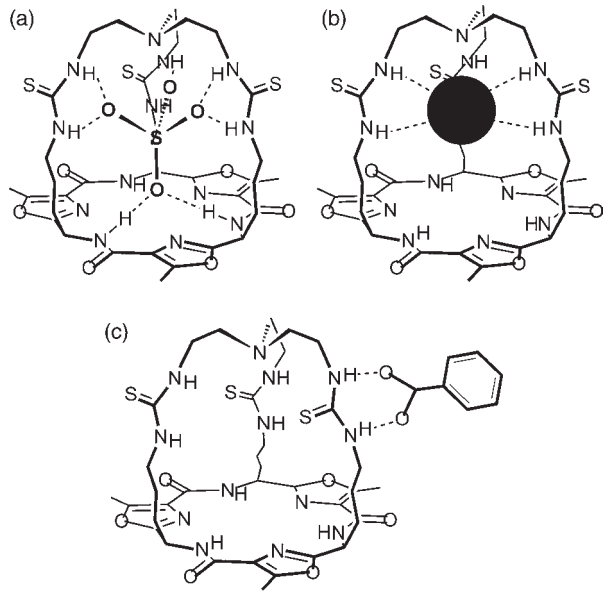

Figure 7. Proposed binding mode of receptor **1** for (a) sulphate anions involving a total of nine hydrogen-bonding interactions; (b) spherical anions involving six hydrogen-bonding interaction and (c) benzoate.

Under these conditions, receptor **1** showed selectivity in the order $SO_4^{2-} \gg Cl^- > AcO^- > Br^-$. Further reductions in binding affinity were observed on moving to an even more competitive environment (20% v/v H_2O/DMSO-d_6). Only modest binding was observed for chloride, bromide and acetate ($K_a = 322$, 38 and $50\,M^{-1}$, respectively), while an apparent stability constant of $1.3 \times 10^3\,M^{-1}$ was observed for sulphate in this solvent mixture. We attribute the strong affinity and selectivity for sulphate in these highly competitive solvent mixtures to the unique binding mode the oxoanion is able to adopt with **1**, given that we observed significant downfield shifts for the signals attributable to the amide protons of **1** in these more polar solvent mixtures, while relatively small upfield shifts of the amide protons were observed for titrations with the remaining anions (Figure 8).

Increasing the water content of the solvent to 25% v/v H_2O/DMSO-d_6 resulted in large decrease in apparent stability constants obtained for both chloride ($K_a = 83\,M^{-1}$) and sulphate ($K_a = 141\,M^{-1}$) and in 35% v/v H_2O/DMSO-d_6 only small changes were observed in ^{1}H NMR spectra resulting in $K_a < 25\,M^{-1}$ for both chloride and sulphate ions. Notably, in 20–25% v/v H_2O/DMSO-d_6 on addition of sulphate ions, the signals for the thiourea protons broadened considerably and could not be used to determine stability constants. A steeper drop off in binding affinity for sulphate then chloride ions was observed on increasing the polarity of the solvent, resulting in a loss of sulphate selectivity in 35% v/v H_2O/DMSO-d_6.

Table 3. Apparent stability constants (K_a/M^{-1}) of **1** towards various anions added as their tetrabutylammonium salts as determined by monitoring the thiourea NH signals (unless specified) during ^{1}H NMR titrations in increasing amounts of H_2O in DMSO-d_6.[a]

Anion	0.5% H_2O[b]	10% H_2O	20% H_2O	25% H_2O	35% H_2O
Cl^-	$>10^4$	2.3×10^3	322	83	25 ($\pm$ 10)
Br^-	2.7×10^3	181	38	nd	nd
AcO^-	$>10^4$	775	50	nd	nd
SO_4^{2-}	$>10^4$	$>10^4$	1.3×10^{3c}	141[c]	13 ($\pm$ 8)

[a] Determined at 330 K. Data were fit to a 1:1 binding model. K_a values are an average of the values obtained by monitoring thiourea (NH^a and NH^b). Errors $<$15% unless specified.
[b] Data from Table 2.
[c] Determined by monitoring the amide (NH^d) proton shifts.

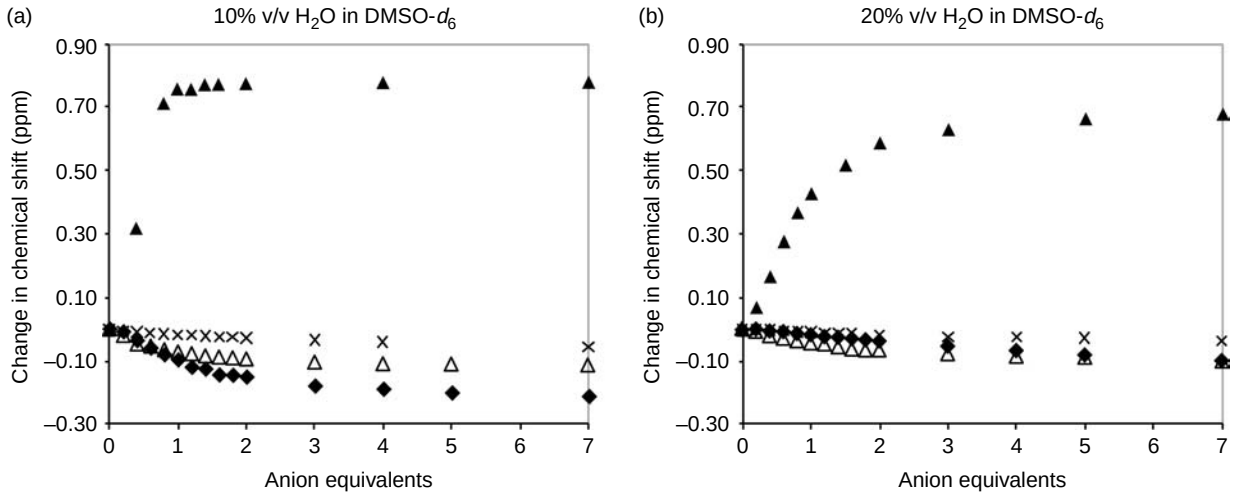

Figure 8. Changes in chemical shift (ppm) of the amide protons of **1** in 10% v/v H_2O/DMSO-d_6 (left) and 20% v/v H_2O/DMSO-d_6 (right) with the addition of various anions. In both cases, the signal shifts downfield with the addition of sulphate (keys: × = bromide, △ = chloride, ◆ = acetate, ▲ = sulphate).

Presumably this is due to the relative hydrophilicities of the two anions, which become more significant as the amount of water in solution is increased (*17*).

Conclusions

Compounds **1** and **2** bind to selected anions strongly in a 1:1 manner in 0.5% H_2O/DMSO-d_6 with both receptors having K_as $> 10^4\,M^{-1}$ for acetate and sulphate in this solvent, while **1** also binds strongly to chloride ions ($K_a > 10^4\,M^{-1}$) and **2** binds strongly to dihydrogen phosphate ions ($K_a > 10^4\,M^{-1}$). Changing the solvent conditions to 10% H_2O enabled the selectivity of **1** to be determined as $SO_4^{2-} \gg Cl^- > AcO^- > Br^-$. The selectivity of **1** for sulphate ions is attributed to binding of this anion via nine hydrogen bonds; six from thioureas and three from the cyclic peptide. In contrast, ^{1}H NMR evidence suggests that chloride and acetate anions do not interact with the cyclic peptide amide protons and are bound through hydrogen-bonding interactions with only the thiourea binding sites. Larger anions that do not fit inside the cavity, such as benzoate, are weakly bound to the exterior of the cryptands. The cyclic peptide scaffolds of these cryptands will be useful in the development of further selective anion receptors. Exploitation of this scaffold in the design of new anion receptors is currently underway in our laboratories.

Experimental

General

Melting points were measured using a Stanford Research Systems Optimelt melting apparatus and are uncorrected. Optical rotations were performed using a Perkin Elmer Model 341 polarimeter using the indicated spectroscopic grade solvents. ^{1}H NMR spectra were recorded using a Bruker Avance DPX 400 at a frequency of 400.13 MHz and are reported as ppm downfield shift from deutero-chloroform ($CDCl_3$, δ_H 7.26 ppm) or DMSO-d_6 (δ_H 2.50 ppm) as internal references, unless otherwise stated. ^{13}C NMR spectra were recorded using a Bruker Avance DPX 400 at a frequency of 100.61 MHz and are reported as ppm downfield shift from deuterochloroform (δ_C = 77.16 ppm) or DMSO-d_6 (δ_C 39.52 ppm) as internal

references, unless otherwise stated. Low-resolution electrospray ionisation (ESI) spectra were recorded by a Thermo Finnigan LCQ Deca Ion Trap mass spectrometer. Reverse-phase preparative HPLC (RP-HPLC) was performed on a Waters 600E multisolvent delivery system with a Waters U6K injector, Waters 490E programmable multiwavelength detector, Waters busSAT/IN module and Waters Empower 2 software. Separation was achieved on a Sunfire™ PrepC_{18} OBD™ column (5 μm, 150 × 19 mm ID). The elution rate was maintained at 7.0 ml/min over the stated linear gradient, comprised of solvent A (100:0.05 Milli-Q water/trifluoroacetic acid (TFA)) and solvent B (100:0.05 acetonitrile/TFA).

Cyclo[Orn(NCS)–Thr(Oxz)]₃ (6)

Under an atmosphere of nitrogen, carbon disulphide (291 μl, 4.83 mmol) was added to a solution of tris-hydrobromide **3b** (200 mg, 0.241 mmol) in dimethylformamide (7.5 ml) and triethylamine (302 μl, 2.17 mmol). Subsequent addition of *N,N′*-DCC (154 mg, 0.748 mmol) was followed by stirring at room temperature for 19 h. The resulting reaction mixture was then concentrated under reduced pressure providing the crude product as a yellow-gold residue that was purified by flash chromatography [silica gel; CH_2Cl_2/EtOAc (12:1)]. Combination of appropriate fractions gave the desired tris-isothiocyanate **6** as a colourless solid (145 mg, 84%). MP: 184–185°C; $[\alpha]_D^{20}$ + 5.65 (c 0.2, $CHCl_3$); ^{1}H NMR (400 MHz, $CDCl_3$): δ (ppm) 8.34 (d, $J = 6.4$, 3H), 5.18–5.12 (m, 3H), 3.59 (t, $J = 6.6$ Hz, 6H), 2.66 (s, 9H), 2.31–2.19 (m, 3H), 2.08–1.87 (m, 6H) and 1.80–1.67 (m, 3H); ^{13}C NMR (100 MHz, $CDCl_3$): δ (ppm) 161.1, 160.5, 154.5, 130.5, 128.4, 47.4, 44.7, 32.0, 25.6 and 11.8; MS (ESI+) $m/z = 734$ $[M + Na]^+$.

General method for the synthesis of cryptands from 6

Under an atmosphere of nitrogen, a solution of tris-isothiocyanate **6** (1 equiv.) in $CHCl_3$ (3.0 mM) and a separate solution of tris-amine (1 equiv.) in $CHCl_3$ (3.0 mM) were added dropwise, via syringe pump (1.5 ml/h), to neat $CHCl_3$ (final concentration 1.0 mM) at reflux. The reaction mixture was allowed to stir at reflux for a further 16 h and was then concentrated under reduced pressure providing an orange residue as the crude product. Purification by column chromatography [silica gel; $CHCl_3$/MeOH/NH_3 (90:9:1)] followed by RP-HPLC gave the desired tris-urea cryptands.

Cryptand 1

Treatment of **6** (30.0 mg, 41.2 μmol) according to the general method and purification by RP-HPLC (5–50% A/95–50% B over 40 min; $t_R = 40.0$ min) gave the desired cryptand **1** as an off-white solid (15.0 mg, 42%). All characterisation data were in agreement with those data that previously reported (*12*).

Cryptand 2

Treatment of **4** (15.0 mg, 21.1 μmol) according to the general method and purification by RP-HPLC (50–100% A/50–0% B over 30 min; $t_R = 25.1$ min) gave the desired cryptand **2** as an off-white solid (3.1 mg, 16%). All characterisation data were in agreement with those data that previously reported (*12*).

Crystal data for 6

Data were collected on a Bruker-Nonius APEX2-X8-FR591 diffractometer employing graphite-monochromated Mo-K_α radiation generated from a rotating anode (0.71073 Å) with ω and φ scans at 150(2) K. Data integration and reduction were undertaken with SAINT and XPREP (*18*). Subsequent computations were carried out using the WinGX-32 graphical user interface (*19*). The structure was solved by direct methods using SIR97 (*20*). Multi-scan empirical absorption corrections were applied to the data-set using the program SADABS (*21*). Data were refined and extended with SHELXL-97 (*22*). Specific details regarding the crystal structure refinement are given below.

Formula: $C_{30}H_{33}N_9O_6S_3$, M 711.83, monoclinic, space group $C2$(#5), a 13.7798(15), b 17.2621(15), c 14.5894(14) Å, β 102.569(5), V 3387.2(6) Å^3, D_c 1.396 g cm^{-3}, Z 4, crystal size 0.20 by 0.03 by 0.01 mm, colourless, habit needle, temperature 150(2) K, λ(Mo-K_α) 0.71073 Å, μ(Mo-K_α) 0.276 mm^{-1}, T(SADABS)$_{min,max}$ 0.6736, 0.7457, $2\theta_{max}$ 46.50, hkl range −15 15, −18 19, −16 16, N 10,993, N_{ind} 4862(R_{merge} 0.0498), N_{obs} 3528($I > 2\sigma(I)$), N_{var} 443, residuals $R_1(F)$ 0.0820, w$R_2(F^2)$ 0.2433, GoF(all) 1.053, $\Delta\rho_{min,max}$ −0.408, 2.105 e$^-$ Å^{-3}.

Specific details. The crystal employed in this study was very small and weakly diffracting. Despite the use of a low temperature device, a high-powered laboratory X-ray source (5 kW) and long exposure times, little diffraction was observed beyond 0.9 Å resolution. In addition, there is some disorder present in the lattice with two of ethylene chains modelled over two positions with occupancies of 0.75 and 0.25, respectively. In one case, this extends to include the thiocyanate group. There is a large residual peak located very close to one of the disordered sulphur atoms (S3A), which is due to adsorption effects and/or unresolved disorder. A number of bond length and angle restraints were required to facilitate realistic modelling. Each of the disordered groups was modelled with identical thermal parameters. The refined Flack parameter

(−0.10(18)) (*16*) confirms the enantiopurity of the cyclic peptide.[1]

Binding studies

Typically, a 1–5 mM stock solution of **1** or **2** was accurately prepared in the stated deuterated solvents (v/v) using a volumetric flask. Solutions of anions to be titrated were then prepared in separate volumetric flasks using the same host solution so that the concentration of the host remained constant throughout a given titration experiment. The concentration of anion solutions was made 50 times that of the host (i.e. 0.1–0.25 M). In each case, 500 μl of host solution in a NMR tube was titrated with aliquots of anion stock solution and after each addition the ^{1}H NMR spectrum was recorded after thorough mixing. Typically, this was obtained in the following order: 10 × 2 μl, 3 × 10 μl, 20 μl and 30 μl (total 100 μl/10 equivalents). Titrations were performed in duplicate.

Nonlinear curve fitting of the experimentally obtained titration isotherms (equivalents of anion vs chemical shift of thiourea or amide protons) using the programme *Equilibria* (*23*) enabled the calculation of apparent stability constants (K_a/M^{-1}). In all cases, the complete dissociation of the tetrabutylammonium salts was assumed and the data were fit to a 1:1 binding model. In the case of titrations performed with **1**, titration experiments were conducted at 330 K due to the broad signals observed below this temperature (see supporting information). The apparent stability constants determined by monitoring the thiourea proton signals are an average of the values obtained independently by monitoring NH^a and NH^b of each receptor. Although more than 0.5% H_2O was used as a cosolvent, the H_2O resonance was suppressed through 'WATER suppression by GrAdient-Tailored Excitation' (WATERGATE) (*24*) so that peaks of interest could be monitored throughout the experiment.

Acknowledgements

We thank Dr Ian Luck (USyd) for technical assistance with NMR and the Australian Research Council for financial support.

Note

1. Crystallographic information files reported in the present manuscript have been deposited with the Cambridge Crystallographic Data Centre as supplementary publication number CCDC 831167. Copies of the data are available free of charge from the CCDC, 12 Union Road, Cambridge, CB2 1EZ, UK (Fax: (+44) 1223 336 033; email: deposit@ccdc.cam.ac.uk).

References

(1) For reviews see: Gale, P.A. *Chem. Soc. Rev.* **2010**, *39*, 3746–3771; Caltagirone, C.; Gale, P.A. *Chem. Soc. Rev.* **2009**, *38*, 520–563; Sessler, J.L.; Gale, P.A.; Cho, W.-S. *Anion Receptor Chemistry*; Royal Society of Chemistry, Cambridge, 2006; Bianchi, A., Bowman James, K., García-España, E., Eds; *Supramolecular Chemistry of Anions*, Wiley-VCH: New York, 1997; Beer, P.D.; Gale, P.A. *Angew. Chem. Int. Ed.* **2001**, *40*, 486–516.

(2) Kubik, S. *Chem. Soc. Rev.* **2010**, *39*, 3648–3663; Kubik, S.; Reyheller, C.; Stüwe, S. *J. Incl. Phenom. Macrocycl. Chem.* **2005**, *52*, 137–187.

(3) Pflugrath, W.; Quiocho, F.A. *Nature* **1985**, *314*, 257–260; Pflugrath, W.; Quiocho, F.A. *J. Mol. Biol.* **1988**, *200*, 163–180; He, J.J.; Quiocho, F.A. *Science* **1991**, *251*, 1479–1481.

(4) Amendola, V.; Bonizzoni, M.; Esteban-Gómez, D.; Fabbrizzi, L.; Licchelli, M.; Sancenón, F.; Taglietti, A. *Coord. Chem. Rev.* **2006**, *45*, 1451–1470.

(5) Steed, J.W. *Chem. Soc. Rev.* **2009**, *38*, 506–519; Amendola, V.; Fabbrizzi, L. *Chem Commun*. **2009**, *45*, 513–531; Pérez, J.; Riera, L. *Chem. Soc. Rev.* **2008**, *37*, 2658–2667; O'Neil, E.J.; Smith, B.D. *Coord. Chem. Rev.* **2006**, *250*, 3068–3080.

(6) Gale, P.A.; Hiscock, J.R.; Moore, S.J.; Caltagirone, C.; Hursthouse, M.B.; Light, M.E. *Chem. Asian J.* **2010**, *5*, 555–561; Fiehn, T.; Goddard, R.; Seidel, R.W.; Kubik, S. *Chem. Eur. J.* **2010**, *16*, 7241–7255; Yoon, D.-W.; Gross, D.E.; Lynch, V.M.; Lee, C.-H.; Bennett, P.C.; Sessler, J.L. *Chem. Commun.* **2009**, *45*, 1109–1111; Dydio, P.; Zielinski, T.; Jurczak, J. *Chem. Commun.* **2009**, *45*, 4560–4562; Reyheller, C.; Kubik, S. *Org. Lett.* **2007**, *9*, 5271–5274; Kubik, S.; Goddard, R. *Proc. Natl Acad. Sci.* **2002**, *99*, 5127–5132; Kubik, S.; Goddard, R.; Kirchner, R.; Nolting, D.; Seidel, J. *Angew. Chem., Int. Ed. Engl.* **2001**, *40*, 2648–2651.

(7) Jia, C.-D.; Wu, B.; Li, S.-G.; Huang, X.-J.; Yang, X.-J. *Org. Lett.* **2010**, *12*, 5612–5615; Jia, C.; Wu, B.; Li, S.; Yang, Z.; Zhao, Q.; Liang, J.; Li, Q.-S.; Yang, X.-J. *Chem. Commun.* **2010**, *46*, 5376–5378; Jia, C.; Wu, B.; Li, S.; Huang, X.; Zhao, Q.; Li, Q.-S.; Yang, X.-J. *Angew. Chem. Int. Ed.* **2010**, *50*, 486–490; Fiehn, T.; Goddard, R.; Seidel, R.W.; Kubik, S. *Chem. Eur. J.* **2010**, *16*, 7241–7255; Gale, P.A.; Hiscock, J.R.; Jie, C.Z.; Hursthouse, M.B.; Light, M.E. *Chem. Sci.* **2010**, *1*, 215–220; Custelcean, R.; Bosano, J.; Bonnesen, P.V.; Kertesz, V.; Hay, B.P. *Angew. Chem. Int. Ed*. **2009**, *48*, 4025–4029; Rodriguez-Decampo, Z.; Pascu, S.I.; Kubik, S.; Otto, S. *J. Am. Chem. Soc.* **2006**, *128*, 11206–11210; Otto, S.; Kubik, S. *J. Am. Chem. Soc.* **2003**, *125*, 7804–7805; Kubik, S.; Kirchner, R.; Nolting, D.; Seidel, J. *J. Am. Chem. Soc.* **2002**, *124*, 12752–12760.

(8) Marcus, Y. *J. Chem. Soc. Faraday Trans.* **1991**, *87*, 2995–2999.

(9) Kang, S.O.; Llinares, J.M.; Day, V.W.; Bowman-James, K. *Chem. Soc. Rev.* **2010**, *39*, 3980–4003.

(10) Amendola, V.; Fabbrizzi, L.; Mosca, L. *Chem. Soc. Rev.* **2010**, *39*, 3889–3915; Li, A.-F.; Wang, J.-H.; Wang, F.; Jiang, Y.-B. *Chem. Soc. Rev.* **2010**, *39*, 3729–3745; Kang, S.O.; Begum Rowshan, A.; Bowman-James, K. *Angew. Chem., Int. Ed.* **2006**, *45*, 7882–7894; Kang, S.O.; Hossain, M.A.; Bowman-James, K. *Coord. Chem. Rev.* **2006**, *250*, 3038–3052. Bondy, C.R.; Loeb, S.J. *Coord. Chem. Rev.* **2003**, *240*, 77–99.

(11) Boyle, M.E.; McCabe, T.; Gunnlaugsson, T. *Supramol. Chem*. **2010**, *22*, 586–597; Brooks, S.J.; Garcia-Garrido, S.E.; Light, M.E.; Cole, P.A.; Gale, P.A. *Chem. Eur. J.* **2007**, *13*, 3320–3329; Brooks, S.J.; Gale, P.A.; Light, M.E. *Chem. Commun.* **2006**, 4344–4346.

(12) Young, P.G.; Clegg, J.K.; Bhadbhade, M.; Jolliffe, K.A. *Chem. Commun.* **2011**, *47*, 463–465.

(13) Wipf, P. In *Alkaloids: Chemical and Biological Perspectives*; Pelletier, S.W., Ed.; Elsevier: Amsterdam, 1998; pp 187–228.
(14) Mink, D.; Mecozzi, S.; Rebek, Jr., J. *Tetrahedron* **1998**, *39*, 5709–5712; Lucke, A.J.; Tyndall, J.D.A.; Singh, Y.; Fairlie, D.P. *J. Mol. Graph. Model.* **2003**, *21*, 341–355; Singh, Y.; Stoermer, M.J.; Lucke, A.J.; Guthrie, T.; Fairlie, D.P. *J. Am. Chem. Soc.* **2005**, *127*, 6563–6572; Butler, S.J.; Jolliffe, K.A. *Org. Biomol. Chem.* **2011**, *9*, 3471–3483; McDonough, M.J.; Reynolds, A.J.; Lee, W.Y.G.; Jolliffe, K.A. *Chem Commun.* **2006**, *41*, 2971–2973; Jolliffe, K.A. *Supramol. Chem.* **2005**, *17*, 81–86; Pintér, A.; Haberhauer, G.; Hyla-Kryspin, I.; Grimme, S. *Chem. Commun.* **2007**, *43*, 3711–3713; Pintér, Á.; Haberhauer, G. *Synlett* **2009**, 3082–3098.
(15) Schnopp, M.; Ernst, S.; Haberhauer, G. *Eur. J. Org. Chem.* **2009**, 213–222.
(16) Flack, H.D. *Acta Cryst.* **1983**, *A39*, 876–881.
(17) Hofmeister, F. *Arch. Exp. Pathol. Pharmacol.* **1888**, *24*, 247–260.
(18) Bruker-Nonius; Bruker AXS Inc: Madison Wisconsin, USA, 2003.
(19) Farrugia, L.J. *J. Appl. Cryst.* **1999**, *32*, 837–838.
(20) Altomare, A.; Burla, M.C.; Camalli, M.; Cascarano, G.L.; Giocavazzo, C.; Gaugliardi, A.; Moliterni, G.C.; Polidori, G.; Spagna, S. *J. Appl. Cryst.* **1999**, *32*, 115–119.
(21) Sheldrick, G.M.; SHELXS-97: Programs for Crystal Structure Solutions. University of Göttingen: Germany, 1996–2008.
(22) Sheldrick, G.M.; SHELXL-97: Programs for Crystal Structure Analysis. University of Göttingen: Göttingen, 1997.
(23) Marjo, C.E. *Equilibria*; Mark Wainwright Analytical Centre, University of New South Wales: Sydney, Australia, 2010. http://www.sseau.unsw.edu.au/Index.htm.
(24) Piotto, M.; Soudek, V.; Sklenar, V. *J. Biomol. NMR* **1992**, *2*, 661–665.